Synthesis of Metallomacrocycle and Coordination Polymers with Pyridine-Based Amidocarboxylate Ligands and Their Catalytic Activities towards the Henry and Knoevenagel Reactions

Anirban Karmakar,* Guilherme M. D. M. Rúbio, M. Fátima C. Guedes da Silva, and Armando J. L. Pombeiro*[a]

The reactions of 3,3′-{(pyridine-2,6-dicarbonyl)bis(azanediyl)}dibenzoic acid (H$_2$L) with zinc(II), cadmium(II), and samarium(III) nitrates were studied, and the obtained compounds, [Zn(1κO:2κO′-L)(H$_2$O)$_2$]$_n$ (1), [Cd(1κO^2:2κO^2-L)(H$_2$O)$_2$]$_2$·6n H$_2$O·n C$_4$H$_8$O$_2$·1.5n DMF (2), and [Sm(1κO:2κO′O′′:3κO′′′-L)(NO$_3$)(H$_2$O)(dmf)]$_n$·n DMF (3), were characterized by elemental analysis, FTIR spectroscopy, thermogravimetric analysis, and X-ray single-crystal diffraction. Compounds 1 and 3 have 1D zigzag- and double-chain-type structures, respectively, whereas 2 features a dinuclear metallomacrocyclic complex. The ligand (L^{2-}) orients in different conformations, that is, syn-syn for 1 and anti-anti for 2 and 3. Compound 1 is the first example in which the syn-syn conformation for this ligand has been observed. These compounds act as heterogeneous catalysts for the nitroaldol (Henry; in water medium) and Knoevenagel condensation reactions of different aldehydes, and the most effective is zinc coordination polymer 1. Recyclability, heterogeneity, and size-selectivity tests were performed, which showed that the catalyst was highly active over at least four recycling runs.

1. Introduction

Coordination polymers are normally described as a group of highly promising functional materials due to their fascinating 1D, 2D, and 3D architectures (not necessarily porous) as well as their widespread application in various areas such as gas storage, molecular sensing, catalysis, and separations.[1] Their synthesis can be carefully designed towards specific structures, topologies, and interesting properties.[2] On the other hand, the synthesis of metallomacrocyclic molecules by using metal-directed self-assembly is a current area of research activity.[3] The design and selection of suitable multidentate ligands and metal ions are quite critical in the construction of self-assembled polymetallic structures.[4] In recent years, marked improvement in the synthesis of coordination polymers and metallomacrocyclic compounds with multidentate aromatic carboxyl-

ate ligands has been accomplished.[5] However, it is still a challenge for chemists to develop efficient synthetic strategies to targeted structures and expected properties.

Recently, various coordination polymers were investigated as adaptable supramolecular platforms to develop heterogeneous catalysts for diverse organic transformations,[6] especially for liquid-phase reactions such as Knoevenagel condensation;[7a–c] cyanosilylation of aldehydes and ketones;[7d–g] Henry reaction;[8] oxidation of alkanes, alcohols, and olefins;[9] Mukaiyama aldol reaction;[10] ring opening of epoxides;[11] and transesterification.[8a, 12] This is mainly due to their unique physical and chemical properties, such as high porosity, catalytic activity, and specific structures with particular functionalities.[13]

The Henry or nitroaldol reaction is one of the most powerful and atom-economic reactions for C−C bond formation from an aldehyde and a nitroalkane.[14] It is widely used for the synthesis of organic compounds of pharmaceutical significance. Often, this reaction is performed in the presence of strong bases, such as alkali metal hydroxides, alkoxides, or amines, which leads to the dehydration of β-nitro alcohols with concomitant formation of a nitroolefin.[15] The development of new catalysts and procedures for the Henry reaction is a matter of current interest, namely, towards the reduction of toxic byproducts and an increase in yield and diastereoselectivity. Although many metal complexes that can homogeneously catalyze this reaction are reported in the literature,[8b,16] such homogeneous systems suffer from the limitations of a common high catalyst loading and the inability to recycle the catalyst.

[a] Dr. A. Karmakar, G. M. D. M. Rúbio, Prof. M. F. C. Guedes da Silva, Prof. A. J. L. Pombeiro
Centro de Química Estrutural
Instituto Superior Técnico
Universidade de Lisboa
Av. Rovisco Pais, 1049-001, Lisbon (Portugal)
E-mail: anirbanchem@gmail.com
        pombeiro@tecnico.ulisboa.pt

On the other hand, Knoevenagel condensation is another useful C—C bond-forming reaction that is widely used for the synthesis of fine chemicals.[17] It is generally catalyzed by Lewis acids or bases and is extensively studied in homogeneous systems.[18] Although some coordination polymers also catalyze this reaction effectively, most of them require high catalyst loadings, high temperatures, and long reaction times.[19]

Moreover, both the Henry and Knoevenagel condensation reactions can be catalyzed by Lewis acids or bases, but a literature survey showed that most metal organic compounds catalyze such reactions by Lewis acidic metal centers, whereas catalytic activity by both Lewis acid–base containing coordination polymers remains scant.[7d, 17g–i] Difficulties in developing such catalysts result from the fact that these groups can easily neutralize each other. Therefore, it remains a challenge to develop heterogeneous catalysts that can promote one-pot Lewis acid–base reactions, for example, the Henry or Knoevenagel condensation. To overcome these challenges, our group recently developed several amide-functionalized coordination polymers, in which the amide group served as a Lewis basic center and the metal served as a Lewis acid; these coordination polymers were shown to be quite effective for catalyzing such reactions.[8] In the present work, we added more Lewis basic sites (amide and pyridine groups) in our ligand system and constructed various coordination compounds with metals having different Lewis acidities in extreme transition-metal groups, that is, Sm^{3+}, Zn^{2+}, and Cd^{2+}, which are hard, border-line, and soft Lewis acids, respectively. We aimed to afford bifunctional coordination polymers that are capable of serving as heterogeneous catalysts for the above reactions in a more efficient manner and to compare the effects of different Lewis acid metal characters.

In this context, we chose 3,3′-{(pyridine-2,6-dicarbonyl)bis(azanediyl)}dibenzoic acid (H_2L) as the source of an organic linker due to the fact that the degree of deprotonation of the carboxylic groups could be easily tuned by changing the reaction conditions, with expected formation of coordination polymers. Moreover, the amide functionality in H_2L could offer additional hydrogen-bonding sites as well as a basic center to the frameworks. Various mono- and multinuclear complexes with interesting architectures and properties and similar types of ligands were recently reported.[20] Moreover, not long ago a few amide-based coordination polymers were shown to act as heterogeneous catalysts for various organic transformations.[6d, e, 8d, e, 12a] Hence, the two main objectives of the current work were as follows: 1) to synthesize coordination polymers by using a pyridine amidocarboxylate-based proligand, namely, 3,3′-{(pyridine-2,6-dicarbonyl)bis(azanediyl)}dibenzoic acid (H_2L), as the linker source and different early and late transition-metal ions under various hydrothermal conditions; 2) to apply the synthesized coordination polymers as heterogeneous catalysts for the Henry and Knoevenagel condensation reactions of different aldehydes; 3) to compare the coordination and catalytic behaviors of metals in extreme transition-metal periodic groups, that is, Zn^{II} and Cd^{II} (with a closed d^{10} shell) in group 12 and the 4f lanthanide Sm^{III} in group 3.

Thus, in the present work, we synthesized such a proligand and constructed two new 1D coordination polymers, namely, [Zn(1κO:2κO′-L)(H$_2$O)$_2$]$_n$ (**1**) and [Sm(1κO:2κO′O′′:3κO′′′-L)-(NO$_3$)(H$_2$O)(dmf)]$_n$·nDMF (**3**), and the dinuclear metallomacrocyclic complex [Cd(1κO^2:2κO^2-L)(H$_2$O)$_2$]$_2$·6nH$_2$O·nC$_4$H$_8$O$_2$·1.5nDMF (**2**). The compounds were characterized by elemental analysis, FTIR spectroscopy, thermogravimetric analysis, and single-crystal and powder X-ray diffraction analyses. Moreover, these coordination polymers contain both Lewis acid and basic centers (pyridyl and amido groups) and are insoluble in common organic solvents, which make them promising candidates for bifunctional heterogeneous catalysis. Thus, we tested their heterogeneous catalytic activity towards the Henry and Knoevenagel reactions of aldehydes under mild conditions.

2. Results and Discussion

2.1. Synthesis and Characterization

In general, we used solvothermal reaction procedures for the syntheses of compounds **1**–**3**. The solvothermal reaction of H_2L with zinc(II) nitrate hexahydrate in the presence of dimethylformamide, methanol, and NH_4OH led to the formation of the 1D coordination polymer [Zn(1κO:2κO′-L)(H$_2$O)$_2$]$_n$ (**1**), whereas upon performing a similar reaction with Sm(NO$_3$)$_3$·6H$_2$O in a mixture of dimethylformamide (DMF) and water, the one-dimensional framework [Sm(1κO:2κO′O′′:3κO′′′-L)(NO$_3$)(H$_2$O)-(dmf)]$_n$·nDMF (**3**) was formed. However, the solvothermal reaction of Cd(NO$_3$)$_2$·4H$_2$O with H_2L in a DMF, 1,4-dioxane, and NH_4OH mixture produced the dinuclear metallomacrocyclic-type complex [Cd(1κO^2:2κO^2-L)(H$_2$O)$_2$]$_2$·6nH$_2$O·nC$_4$H$_8$O$_2$·1.5nDMF (**2**) (Scheme 1).

In the IR spectra of **1**–**3**, the characteristic strong bands of coordinated carboxylate groups appear at $\tilde{v} = 1579$–1550 and 1385-1372 cm^{-1} for the asymmetric and symmetric stretching vibrations, respectively.[21a,b] The bands in the $\tilde{v} = 1680$–1670 cm^{-1} regions are attributed to the C=C stretching frequencies of the aromatic rings, and those in the $\tilde{v} = 1623$–1612 cm^{-1} range are attributed to the stretching frequency of the amide C=O group. To prove the presence of Lewis acidic sties in compound **1**, we performed pyridine adsorption analy-
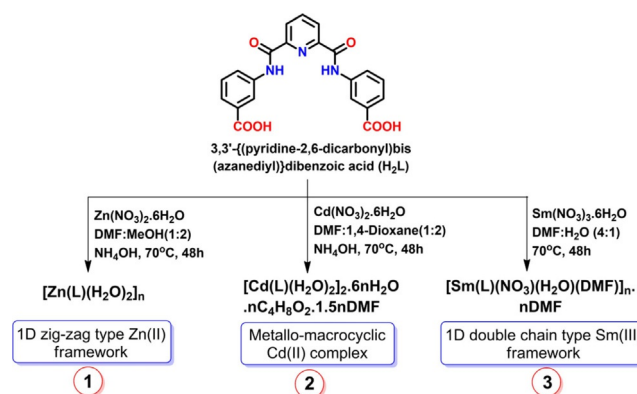
Scheme 1. Reactions of ligand H_2L with Zn, Cd and Sm nitrate salts.

sis and observed a small band at about $\tilde{\nu} = 1443$ cm^{-1}, which is attributed to pyridine adsorption on such sites (Figure S4b, Supporting Information).[21c,d] Due to insolubility in solvents mostly commonly used for NMR spectroscopy, these frameworks were only characterized by infrared spectroscopy, microanalysis, thermogravimetric analysis (Figure S4a), and single-crystal X-ray diffraction.

2.2. Crystal Structure Analysis

The molecular structures of compounds **1–3** were determined by single-crystal X-ray diffraction analysis and are shown in Figures 1–3. Crystallographic data, selected bond lengths and angles, as well as relevant hydrogen-bond contacts are presented in Tables S1–S3, respectively.

Compound **1** crystallizes in the monoclinic C2/c space group, and the asymmetric unit contains one zinc(II) ion, one L^{2-} ligand, and two coordinated water molecules (Figure 1a,b); it features a zigzag-type 1D polymeric chain but expands to 3D by means of H-bond interactions (Figure 1c,d). The zinc center presents a slightly distorted tetrahedral environment ($\tau_4 = 0.92$)[22] made of two water molecules [Zn1—O7, 1.985(14) Å; Zn1—O8, 2.043(15) Å] and two carboxylate oxygen atoms from two L^{2-} units [Zn1—O1, 1.974(8) Å; Zn1—O5,

1.959(9) Å]; each binds the metal in a monodentate fashion. The O—Zn—O bond angles, within the range of 98.8(5) to 117.3(5)°, are similar to those found in the literature.[8a,23] The observed nonplanarity of the organic ligand in **1** may result from the relative twisting of the two CNO amide groups attached to the pyridine ring (dihedral angles of 16.69 and 21.00°), whereas the carboxylate sets are virtually in the plane of the respective phenyl rings (dihedral angles of 3.35 and 9.18°). Due to the conformation of the organic ligand, the Zn^{II} cations are 19.505 Å apart in a chain, a distance that is considerably larger than the shortest intermolecular distance of 6.041 Å between two metal ions in vicinal chains.

In compound **1**, the hydrogen-bond interactions include every amide NH atom, which donates to an amide O atom of a vicinal molecule, and the water molecules, which contact with the noncoordinated carboxylate O atoms. The intermolecular organization in **1** is also characterized by several C—H···O interactions, which helps to expand the structure to the third dimension.

Complex **2** is a dimeric Cd^{II}-based metallomacrocyclic complex (Figure 2a,b) that crystallizes in the triclinic P$\bar{1}$ space group. Its asymmetric unit contains one Cd^{2+} ion, one doubly deprotonated L^{2-} ligand, and two coordinated and three non-coordinated H$_2$O molecules. The Cd^{II} center presents a six-coor-
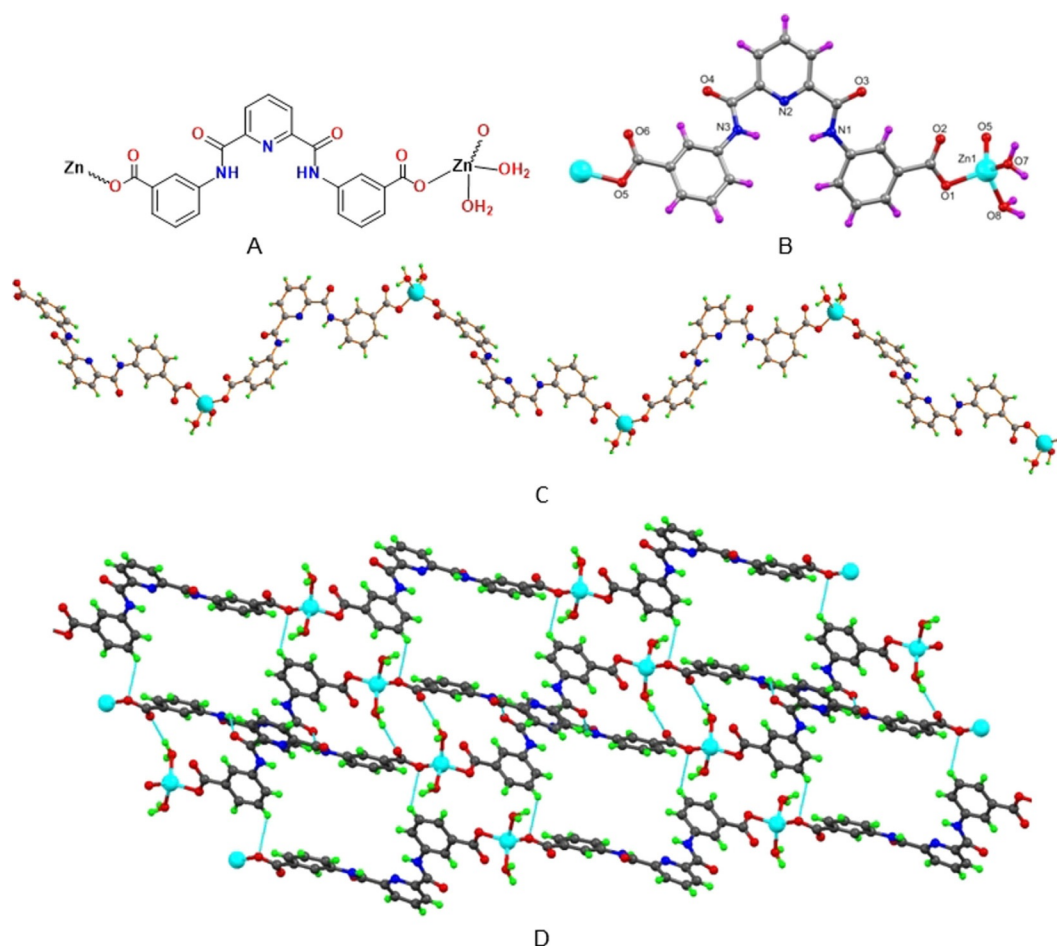

Figure 1. a) Schematic representation, b) molecular structure with partial atom labeling scheme, c) 1D zigzag structure, and d) 3D hydrogen bonded arrangement of compound **1** [Hydrogen bonded pore sizes (7.5 Å X 8.7 Å)].
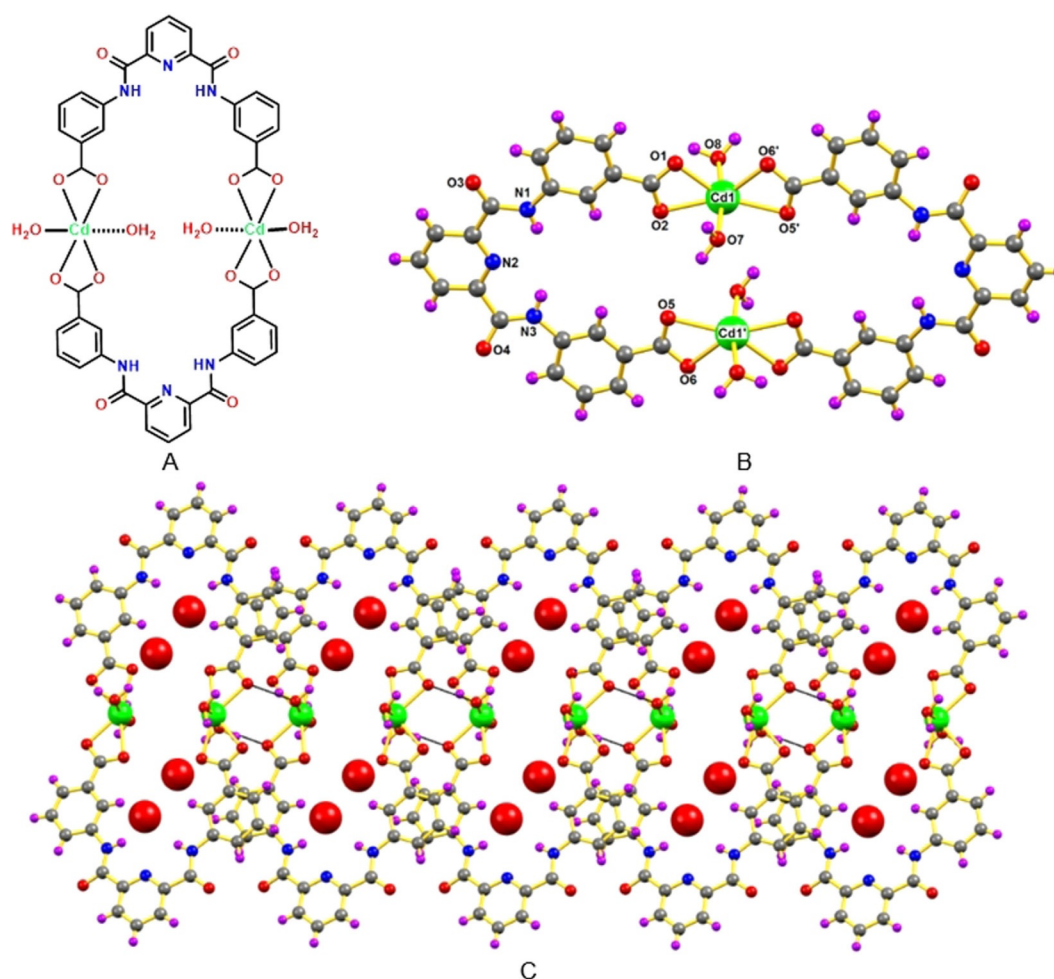
Figure 2. a) Schematic representation, b) crystal structure with partial atom-labeling scheme, and c) hydrogen-bonded packing diagram (the water molecules are presented as a space-filled model) for complex **2**.

dinate environment, in which the four equatorial sites are occupied by two chelating bidentate carboxylate groups from two L^{2-} ligands [Cd1—O1, 2.384(10) Å; Cd1—O2, 2.381(9) Å; Cd1—O5, 2.478(10) Å; Cd1—O6, 2.345(10) Å] and the axial positions engaged with two O atoms from water molecules [Cd1—O7, 2.308(15) Å; Cd1—O8, 2.391(15) Å]. The O—Cd—O bond angles can be as short as 55.3(3)° but reach 171.0(5)° for the almost colinear apical ligands. In view of the binding mode of the carboxylate groups, the deprotonated organic ligand (L^{2-}) is almost planar, as attested by the angle between the least-square planes of the phenyl groups relative to the pyridine ring (2.11 and 7.02°). Regardless of the deviations of the CNO amide groups from the level of the pyridine ring (dihedral angles of 6.82 and 15.30°), the carboxylate sets deviate marginally from the plane of the respective phenyl rings (dihedral angles of 3.41 and 7.28°); 5.469 Å is the intramolecular distance between the Cd^{II} cations, which is very close to the intermolecular one (5.473 Å).

Despite their position towards the inside of the metallacycle ring, the amide NH groups in **2** work as donors to the noncoordinated water molecule [N1—H1···O10 $d_{D-A} = 3.027(14)$ Å, $\measuredangle$ D—H···A 146.4°; N3—H3···O10 $d_{D-A} = 2.920(14)$ Å, $\measuredangle$ D—H···A

154.1°], which, in turn, is also mutually hydrogen bonded with the carboxylates and the coordinated water molecules, therefore expanding the structure to the second dimension (Figure 2 c).

The asymmetric unit of framework **3** contains one Sm^{3+} ion attached to one doubly deprotonated L^{2-} ligand, one bidentate nitrate anion, one DMF molecule, and one water molecule; one noncoordinated DMF molecule is also present in this unit (Figure 3). The organic ligand acts as a bridging tetradentate chelator by means of the carboxylate groups, and each one binds two metals in a bridging bidentate *syn-syn*-type mode. Thus, the Sm^{III} cations participate in a bimetallic 8-membered ($C_2O_4Sm_2$) metallacycle and a monometallic 18-membered ($C_{12}N_3O_2Sm$) metallacycle that share a C—O—Sm boundary. The metal has a coordination number of eight (higher than those of **1** and **2**, as expected), and four of the coordination sites are occupied by the oxygen atoms of the carboxylate groups from four L^{2-} ligands [Sm1—O1, 2.290(4) Å; Sm1—O2, 2.381(4) Å; Sm1—O5, 2.333(4) Å; Sm1—O6, 2.371(4) Å] and two of the coordination sites are occupied by the chelating nitrate anion [Sm1—O7, 2.530(5) Å; Sm1—O8, 2.535(4) Å]; the remaining positions are engaged with a DMF molecule [Sm1—O11,
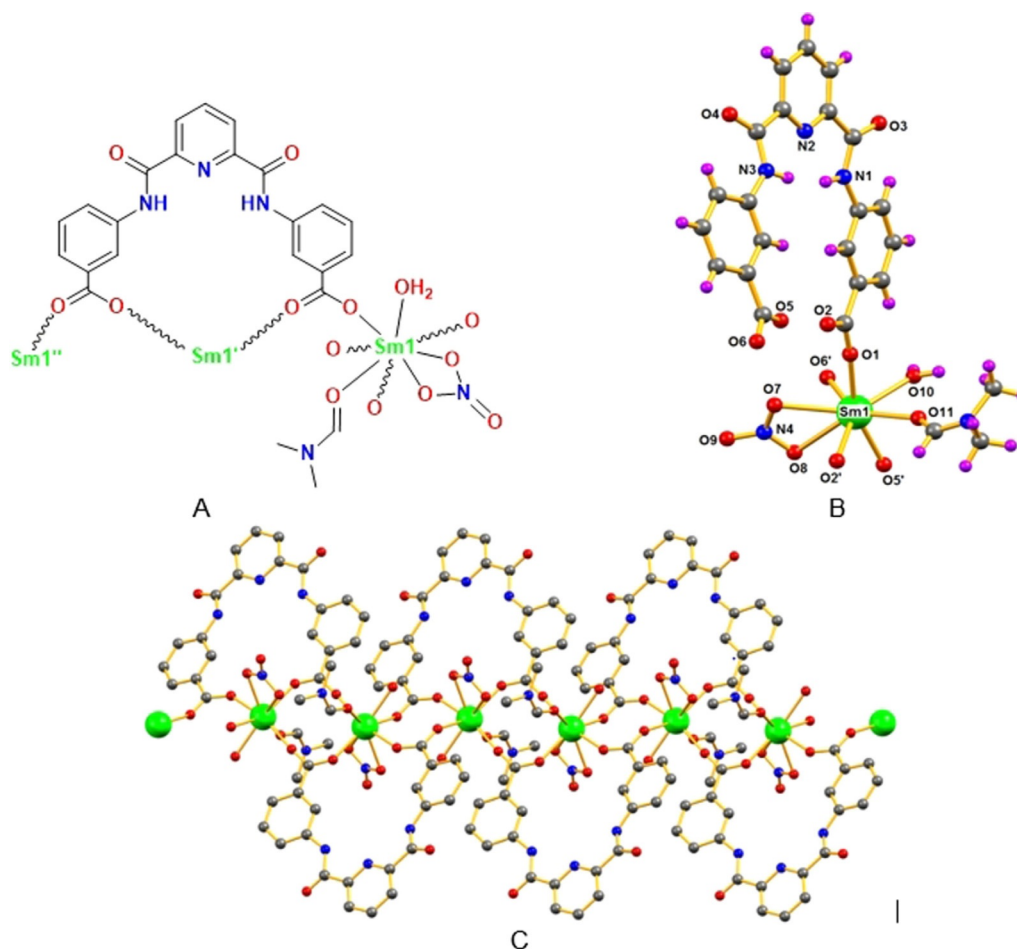
Figure 3. a) Schematic representation, b) molecular structure with partial atom-labeling scheme, and c) 1D structure for framework **3**.

2.385(5) Å] and a water molecule [Sm1–O10, 2.474(4) Å]. The way L^{2-} coordinates to the Sm^{III} ions leads to a double-chain-type 1D coordination polymer. The metal–oxygen bond lengths are within the range of those usually encountered for lanthanide–oxygen assemblies,[8e] and the O–Sm–O bond angles vary from 50.38(17) to 160.40(17)°. Twisting of the L^{2-} ligand in **3** is due not only to the dihedral angles between the amide groups and the pyridine ring (7.98 and 13.49°) but also to those between the carboxylate sets and the related phenyl groups (8.49 and 17.91°). The shortest distance between two Sm^{III} ions in a chain is 5.105 Å, and the shortest distance between vicinal chains is 9.443 Å.

The coordinated water molecules are hydrogen bonded to the O atoms of noncoordinated DMF and to the nitrate group [O10–H10A···O12 $d_{D-A}=2.681(8)$ Å, ∡D–H···A 150°; O10–

H10B···O8 $d_{D-A}=3.055(6)$ Å, ∡D–H···A 155°]. Several C–H···O interactions also help to extend the structure into the third dimension.

Additional to the aforementioned intermolecular interactions, the three assemblies are also stabilized by short π···π interactions of 3.779 (in **1**), 3.565 (in **2**), and 3.611 Å (in **3**), always involving the pyridine and one of the phenyl groups. In such contacts, the rings are mutually parallel but are displaced by angles of 18.5, 21.1, and 19.5°, respectively.

As shown in Scheme 2, three different conformations can exist for the deprotonated ligand L^{2-}, namely, *anti-anti* (in which the carboxylate group and amide O atom orient in an *anti* fashion), *syn-syn* (in which the carboxylate group and amide O atom orient in a *syn* fashion), and *anti-syn*. Recently, Zhou et al. prepared a 3D Cu metal–organic framework (MOF)
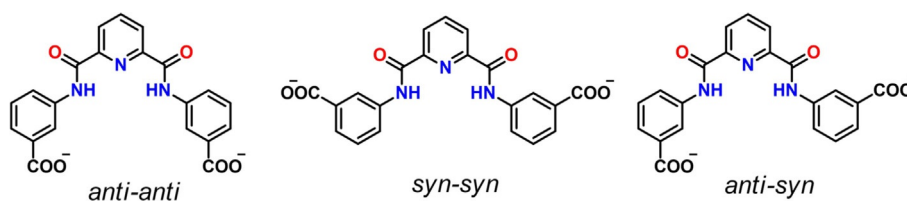
Scheme 2. Three different conformations of L^{2-}.

by using 3,3′-{(pyridine-2,6-dicarbonyl)bis(azanediyl)}dibenzoate (L²⁻) and observed *anti-anti* and *anti-syn* conformations,[20e] but not the *syn-syn* conformation. However, in our case, we obtained the *syn-syn* conformation in the 3,3′-{(pyridine-2,6-dicarbonyl)bis(azanediyl)}dibenzoate ligand (L²⁻) for coordination polymer **1** and the *anti-anti* conformation for compounds **2** and **3**.

Moreover, the carboxylate groups in our L²⁻ ligand can coordinate to the metal centers in various fashions. For example, in the case of compound **1** the carboxylate groups coordinate to the Zn^{II} ions in a monodentate fashion, whereas in **2** they coordinate to the Cd^{II} centers in a chelating mode. For compound **3**, a bridging bidentate fashion is observed.

3. Catalytic Activity

A few amide-based MOFs and coordination polymers have been reported to act as catalysts for the Henry and Knoevenagel condensation reactions.[6d,e,19a,f] The compounds prepared in this study, particularly zinc(II) coordination polymer **1**, have both Lewis acid (Zn²⁺) and basic centers (amide group). Moreover, all of their metal centers show at least two labile ligands (H$_2$O and in the case of **3** also DMF and nitrate). Therefore, they present promising features to act as bifunctional catalysts for these types of reactions. In addition, on account of their insolubility in such solvents, their use as heterogeneous catalysts should be particularly promising.[8]

3.1. Catalytic Activity in the Henry (Nitroaldol) Reaction

We tested the activities of **1–3** as heterogeneous catalysts for the Henry (nitroaldol) reaction of various aldehydes with nitroethane. In a typical reaction, a mixture of benzaldehyde, nitroethane, and 3 mol% catalyst was placed in a glass vessel, and then H$_2$O was added (Scheme 3). The mixture was capped and heated at 70 °C for 48 h, after which it was cooled to room temperature; the solid catalyst was then removed by centrifugation. The products were extracted by using CH$_2$Cl$_2$, which was evaporated under vacuum to give the crude product as a mixture of β-nitroalkanol diastereomers (*syn* and *anti* forms, with predominance of the former; Scheme 3). The diastereomers were analyzed by ^{1}H NMR spectroscopy (Figure S2), and all the obtained results are presented in Table S4.

By using benzaldehyde as a test compound, we found that **1** gave a higher product yield than either **2** or **3** after the same reaction time and temperature. Consequently, optimization of

the reaction conditions (temperature, reaction time, amount of catalyst, solvent) was performed in a model nitroethane–benzaldehyde system with **1** as the catalyst.

Blank reactions were tested with benzaldehyde in the absence of any metal catalyst at 70 °C in water, the reaction yield of nitroalkanol was only 7% after 48 h (Table S4, entry 19). However, the use of proligand H$_2$L led to an overall yield of 10% after 48 h (Table S4, entry 23). We also tested the activities of the nitrate salts of zinc(II), cadmium(II), and samarium(III) and obtained reaction yields in the range of 9 to 11% (Table S4, entries 20–22). The use of 1:1 mixtures of H$_2$L and the Zn^{II}, Cd^{II}, and Sm^{III} salts led to yields between 12 and 17% (Table S4, entries 26–28).

Upon using 3 mol% of **1** as the catalyst, a yield of 72% (*syn/anti* = 62:38) of the β-nitroalkanol from benzaldehyde was reached (Table S4, entry 6). With **2** and **3**, yields of 66 (*syn/anti* = 67:33) and 61% (*syn/anti* = 60:40) were obtained, respectively (Table S4, entries 17 and 18). Extending the reaction time to 72 h did not increase the yield of the reaction. The plot of yield versus time for the Henry reaction of benzaldehyde and nitroethane with coordination polymer **1** is presented in Figure 4a.

We also tested the effect of solvents, amount of catalyst, and temperature in the Henry reaction. An increase in the amount of catalyst **1** from 1.0 to 3.0 mol% enhanced the product yield from 52 to 72% (Table S4, entries 6 and 7), but any further increase in the amount of catalyst did not improve the reaction yield (Table S4, entries 8 and 9).

We performed experiments with various solvents (e.g., CH$_3$CN, THF, MeOH, EtOH, and H$_2$O) with catalyst **1** (Table S4, entries 6 and 10–13) to select the most suitable solvent for this reaction. The results indicated that water (72% yield) was the best solvent, whereas the worst was CH$_3$CN (41% yield) for this catalytic reaction. In THF, methanol, and ethanol, yields of 60, 68, and 63%, respectively, were obtained (Table S4, entries 10–12).

Varying the temperature from 25 to 70 °C improved the yield of the β-nitroalkanol from 10 to 72% (Table S4, entries 6 and 14–16), but any further increase in the reaction temperature had a negative effect (Table S4, entry 16). The *syn* isomer was the major one, and the system typically led to *syn/anti* ratios in the range of 80:20 to 60:40 by using nitroethane as the substrate. The size of the nitroalkane chain also affected the yield, and with nitromethane and nitropropane, yields of 79 and 61%, respectively, were obtained (Table S4, entries 24 and 25).

We also compared the activities of catalyst **1** in the reactions of a variety of substituted aromatic and aliphatic aldehydes with nitroethane to produce the corresponding β-nitroalkanols with yields ranging from 19 to 97% (Table 1). Aryl aldehydes bearing electron-withdrawing groups exhibited higher reactivities (Table 1, entries 1 and 2) than those bearing electron-donating moieties; this may be related to an increase in the electrophilicity of the substrate in the former case.

The efficiency of **1** relative to other previously reported Cu^{II}-, Zn^{II}-, and Sm^{III}-based coordination polymers that have been used as catalysts in the Henry reaction is shown in Table S6.
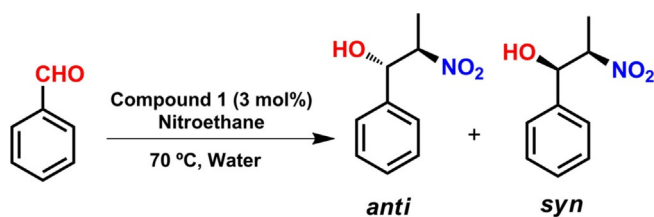
Scheme 3. Henry (nitroaldol) reaction of benzaldehyde with nitroethane and typical conditions.
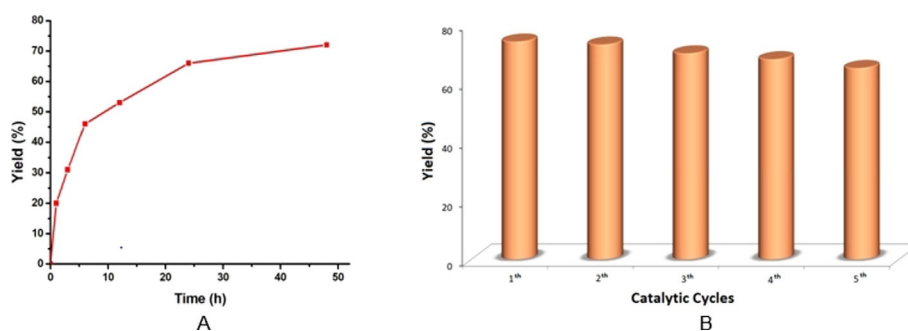
Figure 4. a) Plot of yield versus time for the reaction of benzaldehyde and nitroethane with water as solvent at $T = 70\,°C$ in the presence of catalyst **1**. b) Effect of catalyst recycling on the yield of the β-nitroalkanol resulting from the Henry reaction of benzaldehyde catalyzed by **1**.

Table 1. Henry reaction of various aldehydes and nitroethane with catalyst **1**.[a]

Entry	Aldehyde	Yield[b] [%]	Selectivity[c] (syn/anti)	TON[d]
1	p-nitrobenzaldehyde	93	65:35	31
2	p-chlorobenzaldehyde	67	61:39	22
3	p-methoxybenzaldehyde	19	67:33	7
4	p-methylbenzaldehyde	52	62:38	17
5	p-hydroxybenzaldehyde	60	66:34	20
6	cinnamaldehyde	59	58:42	19
7	acetaldehyde	97	85:15	32

[a] Reaction conditions: catalyst (3.0 mol%), aldehyde (0.5 mmol), nitroethane (0.2 mL, 2.6 mmol), and water (1.0 mL) at 70 °C. [b] Number of moles of β-nitroalkanol per 100 moles of aldehyde. [c] Calculated by ^{1}H NMR spectroscopy. [d] Number of moles of β-nitroalkanol per mole of catalyst.

The reported yields are either lower or comparable to those achieved with **1**. For example, the reaction of 4-nitrobenzaldehyde and nitroethane in the presence of a 3D zinc(II) framework based on 1,3,5-tri(4-carboxyphenoxy)benzene led to an overall yield of only 15% after 72 h (Table S6, entry 4),[24a] whereas a 3D Zn–DABCO (1,4-diazobicyclo[2.2.2]octane) framework produced a higher yield of about 34% after 120 h (Table S6, entry 3);[24b] furthermore, a 2D Zn^{II} coordination polymer of 5-(benzylamino)isophthalate led to a yield of 80% after 48 h at 70 °C by using 10 mol% of the catalyst (Table S6, entry 6).[24c] The same reaction catalyzed by a Cu^{II}–pyridine–2,3,5,6-tetracarboxylate framework led to a yield of 78% after 36 h (Table S6, entry 8).[24f] However, a 2D Zn^{II} framework of 4-(pyridin-4-ylcarbamoyl)benzoate heterogeneously catalyzed the reaction with an overall yield of 93% at 70 °C after 48 h (Table S6, entry 2),[8f] a yield that is identical to that of catalyst **1** (Table S6, entry 1).

For the reaction of unsubstituted benzaldehyde with nitroethane, catalyst **1** gave a product yield (72%) that was similar to that obtained with a Zn^{II} MOF based on 5-{(pyridin-4-ylmethyl)amino}isophthalate[9d] and similar to that obtained with a Sm^{III} MOF based on 2-acetamidoterephthalic acid[8d] (71 and 70%; Table S6, entries 10 and 11).

In our system, interestingly, the reaction yield and the selectivity were higher in an aqueous medium than in an organic solvent, which is not common. The use of an aqueous medium has many advantages owing to the unique properties of water, which include nontoxicity, safety, and environmental benignity. In that context, our complexes are new, effective, recyclable (see below), and environmentally "green" catalysts for the Henry reaction.

The reaction mechanism is expected to be identical to that proposed for related catalytic systems reported by our group.[8d, f, 9d] The Lewis acid center (Zn^{2+}) activates both nitroethane (increasing its acidity) and the aldehyde (increasing its electrophilic character). The amide group and free pyridyl group of the ligand function as a Lewis base, and they assist in deprotonation of acidic nitroethane with the formation of the reactive nitronate species, which adds to the ligated aldehyde through nucleophilic intramolecular attack with formation of a C—C bond, leading to the β-nitroalkanol. Proton abstraction from the nitroalkane and protonation of the C—C coupled species is assisted by the ligand (with carboxylate and amide groups) and also by water, which thus possibly accounts for the good activity of our catalyst in the presence of water.

3.2. Catalytic Activity in the Knoevenagel Condensation Reaction

We tested the catalytic activities of **1**–**3** as heterogeneous catalysts for the Knoevenagel condensation of malononitrile with various aldehydes. In a typical reaction, a mixture of benzaldehyde, malononitrile, and catalyst was placed in a glass vessel, and then THF was added. The mixture was capped and heated at 50 °C for 1.5 h and was subsequently quenched by centrifugation and filtration at room temperature. The filtrate was evaporated under vacuum to give the crude product. The residue was dissolved in CDCl$_3$ and analyzed by ^{1}H NMR spectroscopy. The ^{1}H NMR spectra and calculation of the yield for the Knoevenagel reaction are presented in Figure S3, and all the obtained results are presented in Table S5.

By using benzaldehyde as a test compound (Scheme 4), we found that compound **1** gave a higher product yield than the other catalysts after the same reaction time and at the same temperature. Consequently, optimization of the reaction conditions (temperature, reaction time, amount of catalyst, solvent) was performed in the model malononitrile–benzaldehyde system with **1** as the catalyst.
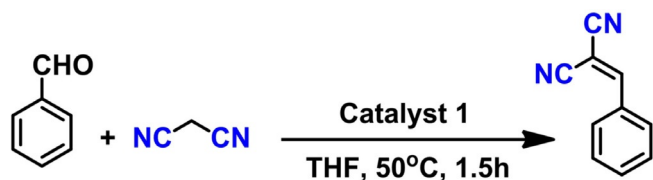
Scheme 4. Knoevenagel condensation reaction of benzaldehyde with malononitrile.

Under the typical conditions of 2 mol% of compound **1** at 50 °C in THF, a yield of 91% of 2-benzylidenemalononitrile was reached (Table S5, entry 4) after 1.5 h. With catalysts **2** and **3**, yields of 84 and 73%, respectively, were obtained (Table S5, entries 13 and 14). Extending the reaction time increased the reaction yield very slowly, and complete conversion was obtained after 6 h. The plot of yield versus time for the Knoevenagel condensation reaction of benzaldehyde and malononitrile with **1** as the catalyst is presented in Figure 5 a.

The effects of temperature, amount of catalyst, and solvents were also tested. An increase in the amount of catalyst **1** from 1.0 to 2.0 mol% enhanced the product yield from 68 to 91%, but any further increase did not lead to any significant increase in catalytic activity (Table S5, entries 4–6).

To select the most suitable solvent, experiments with various solvents (CH_3CN, CH_2Cl_2, THF, MeOH, and EtOH) were performed with coordination polymer **1**. The results (Table S5, entries 7–10) indicated that THF (yield of 91%) was the best solvent, whereas the worst one was CH_3CN (72% yield) for the same reaction time (1.5 h) (Table S5, entries 4 and 7). With methanol, ethanol, and dichloromethane, yields of 89, 83, and 85%, respectively, were obtained (Table S5, entries 8–10) after the same period of time. Increasing the temperature from 25 to 40 °C improved the yield of 2-benzylidenemalononitrile from 43 to 72% (Table S5, entries 11 and 12). A further increase in the temperature to 50 °C enhanced the yield up to 91% (Table S5, entry 4).

Blank reactions were tested with benzaldehyde in the absence of the catalyst at 50 °C in THF and led to a yield of only 24% after 1.5 h (Table S5, entry 15). We also checked the reactivities of $Zn(NO_3)_2 \cdot 6 H_2O$, $Cd(NO_3)_2 \cdot 6 H_2O$, and $Sm(NO_3)_3 \cdot 6 H_2O$

in THF, and the obtained reaction yields were much lower (in the range of 29 to 31%; Table S5, entries 16–18) than those achieved in the presence of catalysts **1–3**. Using 1:1 mixtures of H_2L and zinc nitrate, cadmium nitrate, and samarium nitrate led to yields between 31 and 37% (Table S5, entries 20–22).

We also investigated the catalytic activity of **1** with different types of substituted aromatic and aliphatic aldehydes in the reaction with malononitrile. The results are summarized in Table 2. *p*-Nitro- and *p*-chlorobenzaldehyde produced maximum yields (100–98%), whereas the lowest one (32%) was obtained with *p*-methoxybenzaldehyde, which indicates that an electron-withdrawing substituent promotes the reactivity, in contrast to an electron-donating moiety; this may be related to an increase in the electrophilicity of the substrate in the former case.

Table 2. Knoevenagel condensation reaction of various aldehydes with malononitrile with catalyst **1**.[a]

Entry	Compound	Yield[b] [%]	TON[c]
1	*p*-nitrobenzaldehyde	100	33
2	*p*-chlorobenzaldehyde	98	33
3	*p*-methoxybenzaldehyde	32	11
4	*p*-methylbenzaldehyde	51	17
5	*p*-hydroxybenzaldehyde	48	16
6	cinnamaldehyde	50	17
7	acetaldehyde	92	31

[a] Reaction conditions: catalyst **1** (2.0 mol%), THF (1 mL), benzaldehyde (52 μL, 0.5 mmol), and malononitrile (66 mg, 1.0 mmol). [b] Calculated by ^{1}H NMR spectroscopy. [c] Number of moles of product per mole of catalyst.

A few coordination polymers that are catalytically active for the Knoevenagel condensation reaction of benzaldehyde with malononitrile were reported, but the obtained yields were typically lower or comparable to those obtained with **1** (Table S7).[25] For example, a Zn[II] coordination polymer based on 2,5-dioxidoterephthalate catalyzed the reaction in toluene and produced an overall yield of 77% after 24 h at 70 °C (Table S7, entry 3).[25a] Similarly, a 2D zinc(II) coordination polymer built from the 5-acetamidoisophthalate ligand produced a
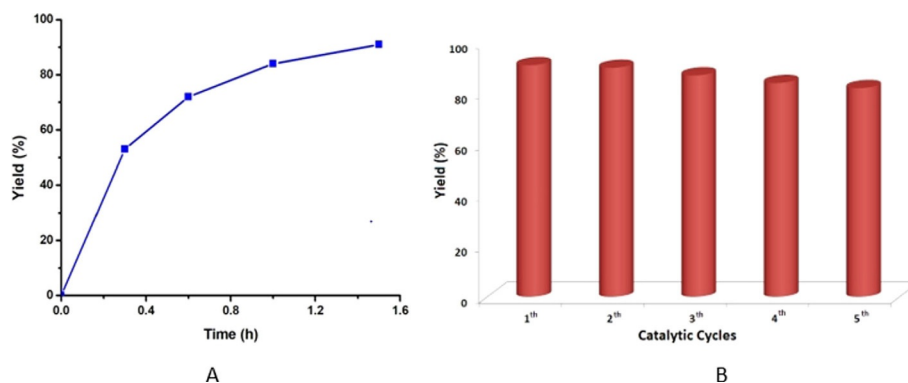

Figure 5. a) Plot of yield versus time for the Knoevenagel condensation reaction of benzaldehyde and malononitrile catalyzed by **1**. b) Effect of catalyst recycling on the yield of 2-benzylidenemalononitrile obtained from the Knoevenagel condensation of benzaldehyde and malononitrile catalyzed by **1**.

61% yield after 1.5 h at 40 °C (Table S7, entry 2).[6e] Moreover, a Ni[II] MOF based on methanetetrabenzoate led to an overall yield of 78% after 6 h at 130 °C (Table S7, entry 6).[25c] A Cd[II] MOF constructed from tri(pyridin-4-yl)cyclohexane-1,3,5-tricarboxamide led to a yield of 80% after 12 h (Table S7, entry 8).[17c] The reaction catalyzed by [Tb(BTATB)(dmf)$_2$(H$_2$O)]$_n$ {BTATB = 4,4′,4′′-[benzene-1,3,5-triyltris(azanediyl)]tribenzoate} produced 99% yield by using 4 mol% of the catalyst at 60 °C for 24 h, that is, a longer time, a higher temperature, and a higher amount of catalyst than in our case (Table S7, entry 7).[17e] With catalyst 1 at 50 °C, a 91% yield was reached in only 1.5 h, and complete conversion was achieved in 3 h. However, a heterometallic Co/Zn MOF based on 5-(picolinamido)isophthalate[17h] led to complete conversion at a lower temperature and a shorter time (Table S7, entry 10). Thus, and according to the above comparisons, catalyst 1 is usually more active than other reported catalysts. In addition, our catalyst is cheap, easy to prepare, highly active at low temperatures, and recyclable without any appreciable loss in activity.
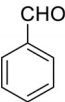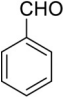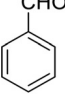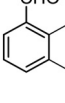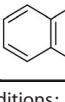
The catalytic process is assumed to follow a mechanism similar to that of the Henry reaction (see above), by which the zinc Lewis acid center interacts with the carbonyl group of benzaldehyde, increasing the electrophilic character of the carbonyl carbon atom. The interaction of a cyano group of malononitrile with the Lewis acid metal site increases the acidity of its methylene moiety. The basic sites (carboxylate O atom, amide N atom, or pyridyl N atom) can abstract a proton from the methylene group to generate the corresponding nucleophilic species, which attacks the carbonyl group of coordinated benzaldehyde with C−C bond formation and dehydration.

For both catalytic reactions, the relationship between structure and catalytic activity in the present study is not clearly understood, but both the metal ion and the structural arrangement affect the catalytic activity. For both reactions, compound 1 afforded the highest yield, and compound 3 afforded the lowest one. The former case is consistent with the high Lewis acidic character of Zn[II] and with its highest coordinative unsaturation and least crowded coordination environment (tetrahedral). In contrast, the lowest yield for compound 3 corresponds to the highest crowded octacoordinated environment around Sm[III]. Moreover, conceivably due to the presence of both free basic sites (amide N atom and pyridyl N atom) and to its simple 1D structure, coordination polymer 1 led to reaction yields that were higher or similar to the reported ones.

3.3. Size-Selectivity Studies

To test the size selectivity of 1 for the Henry and Knoevenagel reactions, we varied the size and shape of the aldehydes, nitroalkanes, and active methylene compounds (Table 3). The aldehydes used were as follows: benzaldehyde (4.8 Å×5.9 Å), naphthaldehyde (5.9 Å×7.0 Å), and 9-anthraldehyde (6.0 Å× 9.3 Å).[9d] The nitroalkanes were nitromethane (2.0 Å×3.3 Å), nitroethane (2.2 Å×3.9 Å), and nitropropane (2.2 Å×5.6 Å),[9d] whereas the active methylene compounds were malononitrile (4.5 Å×6.9 Å), ethyl cyanoacetate (4.5 Å×10.3 Å), and tert-butyl cyanoacetate (5.8 Å×10.3 Å).[9d] We observed that the reaction yield systematically decreased with an increase in the molecular size of the substrates. For example, the reaction of benzaldehyde with nitropropane led to a yield of 61%, which is lower than the yield of 79% for nitromethane (Table 3, entries 3 and 1). In the case of nitroethane, the yield was 72% (Table 3, entry 2). The yields of 1-naphthaldehyde and 9-antraldehyde (with molecular sizes that hamper their fitting into the catalyst cavities) were reduced to 53 and 37%, respectively, under the same reaction conditions (Table 3, entries 4 and 5).

Table 3. Henry reaction[a] and Knoevenagel condensation[b] of substrates of different sizes catalyzed by 1.

Entry	Aldehyde	Nitroalkane	Yield [%]	Entry	Active methylene compound	Yield [%]
1	CHO (benzaldehyde)	nitromethane	79	6	malononitrile	91
2	CHO (benzaldehyde)	nitroethane	72	7	ethyl cyanoacetate	73
3	CHO (benzaldehyde)	nitropropane	61	8	tert-butyl cyanoacetate	45
4	CHO (naphthaldehyde)	nitroethane	53	9	malononitrile	82
5	CHO (anthraldehyde)	nitroethane	37	10	malononitrile	67

[a] Reaction conditions: catalyst 1 (3.0 mol%), benzaldehyde (52 μL, 0.5 mmol), nitroethane (0.2 mL, 2.6 mmol), and water (1.0 mL) for 48 h at 70 °C. [b] Reaction conditions: catalyst (2.0 mol%), THF (1 mL), malononitrile (66 mg, 1.0 mmol), and benzaldehyde (52 μL, 0.5 mmol) for 1.5 h at 50 °C.

We also observed a similar phenomenon in the case of the Knoevenagel reaction: upon increasing the size of the active methylene compound (malononitrile < ethyl cyanoacetate < tert-butyl cyanoacetate) or the aldehyde (benzaldehyde < 1-naphthaldehyde < 9-antraldehyde), the yield decreased from 91 to 45 % (Table 3, entries 6 and 8) or from 91 to 67 % (Table 3, entries 6, 9 and 10), respectively.

These results suggest that both reactions catalyzed by **1** are dependent on its hydrogen-bonded pore sizes (7.5 Å × 8.7 Å). Larger substrates are less reactive owing to difficulties associated with diffusion into the channels of **1**. These size-selective behaviors support the assumption that catalysis also occurs at the interior catalytic sites and not only at the exterior ones.

3.4. Recyclability and Heterogeneity Tests

We performed recycling experiments of **1** in both the Henry and Knoevenagel reactions. The catalyst, separated by centrifugation of the supernatant solution, was washed with methanol or THF and dried in air. It was then recycled in five consecutive experiments, and only a considerable decrease in yield was observed over the fourth to fifth cycles in either case. The FTIR spectra of catalyst **1** taken before and after the reaction suggested that the structure of the solid was retained (Figure S1 b). This was confirmed by powder XRD, also performed before and after the Henry and Knoevenagel reactions (Figure S1 a). Additionally, the filtrate solution, obtained after separation of the catalyst, was evaporated to dryness, and the amount of zinc was determined to be only between 0.015 and 0.018 % of the amount used in the reaction, which thus ruled out any significant leaching of the catalyst.

To verify further the heterogeneity of the system, a procedure similar to that described by Lempers and Sheldon was followed.[26] The catalytic reaction was started, and at a time when catalyst **1** was most active, it was removed by centrifugation; the catalyst-free solution was kept under the same conditions and was monitored with time. An increase in the yield would indicate continuation of the catalytic reaction and, thus, dissolution of the catalyst. In this experiment, catalyst **1** was removed by centrifugation once the conversion reached about 48 % (after a 6 h reaction time) for the Henry reaction and roughly 53 % (after a 0.3 h reaction time) for the Knoevenagel reaction, whereupon the supernatant fluid was stirred for an additional time under the same reaction conditions. As no further conversion into the product was observed in either case, the tests demonstrated that **1** was heterogeneous in nature.

4. Conclusions

We successfully synthesized and characterized three coordination compounds of zinc (**1**), cadmium (**2**), and samarium (**3**) derived from 3,3′-{(pyridine-2,6-dicarbonyl)bis(azanediyl)}dibenzoic acid (H₂L). Single-crystal X-ray diffraction analysis revealed that **1** and **3** are coordination polymers having zigzag- and double-chain-type one-dimensional structures, respectively, whereas **2** features a dinuclear metallacyclic complex. This

type of ligand is very useful to construct coordination polymers having various architectures with either early (Sm^{3+}) or late (Zn^{2+}, Cd^{2+}) transition metals. Moreover, for the first time, we observed the *syn-syn* (for compound **1**) conformation of such a ligand.

We tested the heterogeneous catalytic activity of the compounds towards the Henry C—C coupling and Knoevenagel condensation reactions of various aldehydes and found that, in both cases, Zn^{II} coordination polymer **1** was the most effective catalyst, conceivably on account of the higher Lewis acid character and lower coordination number of the metal ion. Zn^{II} is a border-line hard/soft Lewis acid, whereas the hard and soft characters of Sm^{III} and Cd^{II}, respectively, do not appear to constitute more favorable features in our case, although any attempt for generalization should not be proposed. Size-selectivity studies indicated that the reaction yield decreased with an increase in the molecular size of the substrates, which supports the assumption that catalysis also occurs at the interior pores of the hydrogen-bonded network. In addition, the stability of catalyst **1** in both reactions was well established, proving that such a coordination polymer could be used as an effective and recyclable heterogeneous catalyst in significant types of reactions, which deserve to be further explored.

Experimental Section

General Methods

The synthetic work was performed in air and at relatively high temperatures. All chemicals were obtained from commercial sources and were used as received. The infrared spectra (4000–400 cm^{-1}) were recorded with a Bruker Vertex 70 instrument in KBr pellets (s = strong, m = medium, w = weak, bs = broad and strong, mb = medium and broad). Carbon, hydrogen, and nitrogen elemental analyses were performed by the Microanalytical Service of the Instituto Superior Técnico. Thermal properties were analyzed with a PerkinElmer Instrument system (STA6000) at a heating rate of 5 °C min^{-1} under a dinitrogen atmosphere. Powder X-ray diffraction (PXRD) was conducted with a D8 Advance Bruker AXS (Bragg Brentano geometry) theta-2-theta diffractometer, with copper radiation (CuKα, λ = 1.5406 Å) and a secondary monochromator, operated at 40 kV and 40 mA. The flat-plate configuration was used, and the typical data collection range was between 5 and 40°. For pyridine adsorption studies, the FTIR spectrum of the solid was recorded with an Agilent Cary 630 FTIR spectrometer in the 4000–400 cm^{-1} wavenumber range by using the diffuse reflectance infrared Fourier transform (DRIFT) technique. For acidity determinations by FTIR spectroscopy, the sample was heated to 100 °C under vacuum at around 10^{-5} torr for 12 h. Pyridine adsorption was performed at room temperature for 4 h. The sample was then evacuated for 1 h at 100 °C and was cooled to room temperature before recording the spectrum.

Syntheses

Compound 1: A solution of H₂L (10.1 mg, 0.025 mmol) and zinc(II) nitrate hexahydrate (14.9 mg, 0.050 mmol) in DMF/MeOH (1:2, 2 mL) and containing 30 % ammonium hydroxide (NH₄OH) solution (0.5 mL) was prepared and then transferred to a 8 mL glass vessel, which was sealed and heated at 70 °C for 48 h (solvothermal reac-

tor). Cooling of the solution to room temperature afforded small colorless crystals of **1**. FTIR (KBr): $\tilde{\nu} = 3372$ (s), 3298 (bs), 3188 (s), 2362 (w), 1680 (s), 1665 (s), 1612 (s), 1579 (s), 1476 (m), 1440 (s), 1372 (s), 1321 (m), 1261 (s), 1145 (m), 1080 (m), 1001 (m), 944 (m), 822 (s), 769 (s), 748 (s), 675 (s), 595 (w), 538 (w), 426 cm^{-1} (w); elemental analysis calcd (%) for $C_{21}H_{17}N_3O_8Zn$ (504.74): C 49.97, H 3.39, N 8.32; found: C 49.53, H 3.45, N 8.65.

Compound **2**: A solution of H_2L (10.1 mg, 0.025 mmol) and cadmium(II) nitrate hexahydrate (15.4 mg, 0.050 mmol) in DMF/dioxane (1:2, 2 mL) and containing 30% NH_4OH solution (0.5 mL) was prepared and then transferred to a 8 mL glass vessel, which was sealed and heated at 70 °C for 48 h (solvothermal reactor). Cooling of the solution to room temperature afforded light-yellow crystals of **2**. FTIR (KBr): $\tilde{\nu} = 3446$ (b), 3153 (s), 1665 (m), 1619 (s), 1561 (s), 1409 (s), 1380 (s), 1170 (w), 1083 (m), 1014 (w), 894 (w), 776 (m), 681 (m), 572 (w), 437 cm^{-1} (w); elemental analysis calcd (%) for $C_{50.5}H_{64.5}Cd_2N_{7.5}O_{25.5}$ (1409.41): C 43.04, H 4.61, N 7.45; found: C 43.13, H 4.45, N 7.32.

Compound **3**: A solution of H_2L (10.1 mg, 0.025 mmol) and samarium(III) nitrate hexahydrate (22.2 mg, 0.050 mmol) in DMF (2 mL) and water (0.5 mL) was prepared and then transferred to a 8 mL glass vessel, which was sealed and heated at 70 °C for 48 h (solvothermal reactor). Cooling of the solution to room temperature afforded colorless crystals of **3**. FTIR (KBr): $\tilde{\nu} = 3853$ (w), 3347 (mb), 1670 (m), 1623 (s), 1550 (s), 1407 (s), 1385 (s), 1160 (w), 1079 (m), 1003 (w), 890 (w), 773 (m), 754 (m), 673 (m), 574 (w), 435 cm^{-1} (w); elemental analysis calcd (%) for $C_{27}H_{29}N_6O_{12}Sm$ (779.91): C 41.58, H 3.75, N 10.78; found: C 41.43, H 3.20, N 10.34.

Procedure for the nitroaldol (Henry) reaction: In a typical reaction, a mixture of aldehyde (1 mmol), nitroethane (0.3 mL), and complex **1** (5.6 mg, 3 mol%) was placed in a capped glass vessel; then, water (2 mL) was added. The mixture was heated at 70 °C for 48 h, and the reaction was subsequently quenched by centrifugation and filtration. The filtrate was extracted with dichloromethane. The organic extracts were collected over anhydrous sodium sulfate; subsequent evaporation of the solvent gave the crude product. The residue was dissolved in $CDCl_3$ and analyzed by ^1H NMR spectroscopy. The yield of the β-nitroalkanol product (relative to the aldehyde) was established typically by taking into consideration the relative amounts of these compounds, as given by ^1H NMR spectroscopy and previously reported.[8] The *syn/anti* selectivity was calculated on the basis of the ^1H NMR spectra (Figure S7). In the ^1H NMR spectra, the values of the vicinal coupling constants (for the β-nitroalkanol products) between the α-N—C—H and the α-O—C—H protons identified the isomers, that is, $J = 7–9$ and 3.2–4 Hz for the *syn* and *anti* isomers, respectively.[27]

To perform the recycling experiment, the catalyst isolated by filtration was first washed and dried. It was then used in the nitroaldol reaction as described above.

Procedure for the Knoevenagel condensation reaction: A mixture of benzaldehyde (51 μL, 0.50 mmol), malononitrile (66 mg, 1.0 mmol), and catalyst (5.0 mg of **1**, 12.1 mg of **2**, 7.8 mg of **3**; 2 mol%) was placed in a capped glass vessel, and then THF (1 mL) was added. The mixture was heated at 50 °C for 1.5 h, and the reaction was subsequently quenched by centrifugation and filtration at room temperature. The filtrate was evaporated under vacuum to give the crude product [2-(phenylmethylene)malononitrile]. The residue was dissolved in $CDCl_3$ and analyzed by ^1H NMR spectroscopy. An example of the ^1H NMR spectrum is presented in Figure S2, and the reaction yield was calculated on the basis of previous literature.[6d,e]

To perform the catalyst recycling experiments, the used catalyst (separated by centrifugation of the supernatant solution) was washed with THF and dried in air. It was then reused for the Knoevenagel condensation reaction as described above.

Crystal Structure Determination

X-ray-quality single crystals of compounds **1**–**3** were immersed in cryo-oil, mounted in a nylon loop, and measured at room temperature. Intensity data were collected by using a Bruker APEX-II PHOTON 100 diffractometer with graphite monochromated MoKα ($\lambda = 0.71069$) radiation. Data were collected by using phi and omega scans of 0.5° per frame, and a full sphere of data was obtained. Cell parameters were retrieved by using Bruker SMART[28a] software and were refined by using Bruker SAINT[28a] on all the observed reflections. Absorption corrections were applied by using SADABS.[28b] Structures were solved by direct methods by using the SHELXS-2014 package[28c] and were refined with SHELXL-2014/6.[28c] Calculations were performed by using the WinGX System-Version 2014.1.[28d] The hydrogen atoms attached to carbon and nitrogen atoms were inserted at geometrically calculated positions and were included in the refinement by using the riding-model approximation; $U_{iso}(H)$ was defined as $1.2\,U_{eq}$ of the parent atoms for the phenyl groups and $1.5\,U_{eq}$ of the parent atoms for the methyl groups and nitrogen atoms. Least-square refinements with anisotropic thermal motion parameters for all the non-hydrogen atoms and isotropic ones for the remaining atoms were employed. Compound **2** contained disordered and 1,4-dioxane (1,4-diox) molecules that could not be modeled reliably. PLATON/SQUEEZE[28e] was used to correct the data, and a potential volume of 217 Å^3 was found with 108 electrons per unit cell worth of scattering. The electron count suggest the presence of one 1,4-dioxane molecule (48 electrons) per asymmetric unit. Elemental and thermogravimetric analysis data also support this result. These were removed from the model and included in the empirical formula. Crystallographic data are summarized in Table S1, and selected bond lengths and angles are presented in Table S2.[29]

Conflict of Interest

The authors declare no conflict of interest.

[1] a) A. Schoedel, M. Li, D. Li, M. O'Keeffe, O. M. Yaghi, *Chem. Rev.* **2016**, *116*, 12466–12535; b) H.-C. Zhou, S. Kitagawa, *Chem. Soc. Rev.* **2014**, *43*, 5415–5418; c) Z. Zhang, M. J. Zaworotko, *Chem. Soc. Rev.* **2014**, *43*, 5444–5455; d) W. Liu, L. Zhu, Y. Jiang, X.-Q. Liu, L.-B. Sun, *Chem. Mater.* **2018**, *30*, 1686–1694; e) L.-B. Sun, X.-Q. Liu, H.-C. Zhou, *Chem. Soc. Rev.*

2015, *44*, 5092 – 5147; f) A. Dhakshinamoorthy, H. Garcia, *Chem. Soc. Rev.* **2014**, *43*, 5750 – 5765; g) O. R. Evans, W. Lin, *Acc. Chem. Res.* **2002**, *35*, 511 – 522; h) L. Zhu, X.-Q. Liu, H.-L. Jiang, L.-B. Sun, *Chem. Rev.* **2017**, *117*, 8129 – 8176; i) J. Kou, C. Lu, J. Wang, Y. Chen, Z. Xu, R. S. Varma, *Chem. Rev.* **2017**, *117*, 1445 – 1514; j) A. Karmakar, A. Paul, A. J. L. Pombeiro, *CrystEngComm* **2017**, *19*, 4666 – 4695.

[2] a) B. Li, H.-M. Wen, Y. Cui, W. Zhou, G. Qian, B. Chen, *Adv. Mater.* **2016**, *28*, 8819 – 8860; b) B. Li, M. Chrzanowski, Y. Zhang, S. Ma, *Coord. Chem. Rev.* **2016**, *307*, 106 – 129; c) V. Guillerm, D. Kim, J. F. Eubank, R. Luebke, X. Liu, K. Adil, M. S. Lah, M. Eddaoudi, *Chem. Soc. Rev.* **2014**, *43*, 6141 – 6172; d) Q.-L. Zhu, Q. Xu, *Chem. Soc. Rev.* **2014**, *43*, 5468 – 5512; e) A. Karmakar, I. Goldberg, *CrystEngComm* **2011**, *13*, 350 – 366; f) A. Karmakar, H. M. Titi, I. Goldberg, *Cryst. Growth Des.* **2011**, *11*, 2621 – 2636; g) A. Karmakar, I. Goldberg, *CrystEngComm* **2011**, *13*, 339 – 349; h) A. F. Akbari, G. Mahmoudi, A. V. Gurbanov, F. I. Zubkov, F. Qu, A. Gupta, D. A. Safin, *Dalton Trans.* **2017**, *46*, 14888 – 14896; i) G. Mahmoudi, S. K. Seth, A. Bauzá, F. I. Zubkov, A. V. Gurbanov, J. White, V. Stilinović, Th. Doert, A. Frontera, *CrystEngComm* **2018**, *20*, 2812 – 2821.

[3] a) L. F. Lindoy, K.-M. Park, S. S. Lee, *Chem. Soc. Rev.* **2013**, *42*, 1713 – 1727; b) A. Patra, S. K. Saha, T. K. Sen, L. Carrella, G. T. Musie, A. R. Khuda-Bukhsh, M. Bera, *Eur. J. Inorg. Chem.* **2014**, 5217 – 5232; c) L. M. Mesquita, V. André, C. V. Esteves, T. Palmeira, M. N. Berberan-Santos, P. Mateus, R. Delgado, *Inorg. Chem.* **2016**, *55*, 2212 – 2219; d) V. K. Singh, R. Kadu, H. Roy, P. Raghavaiah, S. M. Mobin, *Dalton Trans.* **2016**, *45*, 1443 – 1454; e) F. Yu, F. Li, J. Hu, L. Bai, Y. Zhu, L. Sun, *Chem. Commun.* **2016**, *52*, 10377 – 10380.

[4] a) C. Zhang, L. Sun, Y. Yan, Y. Liu, Z. Liang, Y. Liu, J. Li, *J. Mater. Chem. C* **2017**, *5*, 2084 – 2089; b) Y. Qi, Y. Luan, J. Yu, X. Peng, G. Wang, *Chem. Eur. J.* **2015**, *21*, 1589 – 1597; c) K. Cai, N. Zhao, N. Zhang, F.-X. Sun, Q. Zhao, G.-S. Zhu, *Nanomaterials* **2017**, *7*, 88; d) Y. Cui, B. Li, H. He, W. Zhou, B. Chen, G. Qian, *Acc. Chem. Res.* **2016**, *49*, 483 – 493.

[5] a) Z.-J. Lin, J. Lü, M. Hong, R. Cao, *Chem. Soc. Rev.* **2014**, *43*, 5867 – 5895; b) L. Yang, L. Cao, X. Li, C. Qin, L. Zhao, K.-Z. Shao, Z.-M. Su, *Dalton Trans.* **2017**, *46*, 7567 – 7576; c) Y. Bai, Y. Dou, L.-H. Xie, W. Rutledge, J.-R. Li, H.-C. Zhou, *Chem. Soc. Rev.* **2016**, *45*, 2327 – 2367; d) J.-P. Zhang, Y.-B. Zhang, J.-B. Lin, X.-M. Chen, *Chem. Rev.* **2012**, *112*, 1001 – 1033.

[6] a) A. Dhakshinamoorthy, A. M. Asiri, M. Alvaro, H. Garcia, *Green Chem.* **2018**, *20*, 86 – 107; b) A. Dhakshinamoorthy, Z. Li, H. Garcia, *Chem. Soc. Rev.* **2018**, https://doi.org/10.1039/C8CS00256H; c) Y.-B. Huang, J. Liang, X.-S. Wang, Rong Cao, *Chem. Soc. Rev.* **2017**, *46*, 126 – 157; d) L. Jiao, Y. Wang, H.-L. Jiang, Q. Xu, *Adv. Mater.* **2018**, *30*, 1703663; e) Z. Hu, D. Zhao, *CrystEngComm* **2017**, *19*, 4066 – 4081; f) Y.-S. Kang, Y. Lu, K. Chen, Y. Zhao, P. Wang, W.-Y. Sun, *Coord. Chem. Rev.* **2018**, https://doi.org/10.1016/j.ccr.2018.02.009.

[7] a) H. Ghasempour, A. A. Tehrani, A. Morsali, J. Wang, P. C. Junk, *CrystEngComm* **2016**, *18*, 2463 – 2468; b) A. Karmakar, A. Paul, K. T. Mahmudov, M. F. C. Guedes da Silva, A. J. L. Pombeiro, *New J. Chem.* **2016**, *40*, 1535 – 1546; c) A. Karmakar, G. M. D. M. Rúbio, M. F. C. Guedes da Silva, S. Hazra, A. J. L. Pombeiro, *Cryst. Growth Des.* **2015**, *15*, 4185 – 4197; d) G. Kumar, R. Gupta, *Inorg. Chem.* **2013**, *52*, 10773 – 10787; e) R. F. de Luis, M. K. Urtiaga, J. L. Mesa, E. S. Larrea, M. Iglesias, T. Rojo, M. I. Arriortua, *Inorg. Chem.* **2013**, *52*, 2615 – 2626; f) A. Karmakar, S. Hazra, M. F. C. Guedes da Silva, A. J. L. Pombeiro, *Dalton Trans.* **2015**, *44*, 268 – 280; g) A. Karmakar, A. Paul, G. M. D. M. Rúbio, M. F. C. Guedes da Silva, A. J. L. Pombeiro, *Eur. J. Inorg. Chem.* **2016**, 5557 – 5567.

[8] a) A. Karmakar, M. F. C. Guedes da Silva, A. J. L. Pombeiro, *Dalton Trans.* **2014**, *43*, 7795 – 7810; b) A. Karmakar, S. Hazra, M. F. C. Guedes da Silva, A. J. L. Pombeiro, *New J. Chem.* **2014**, *38*, 4837 – 4846; c) A. Karmakar, C. L. Oliver, S. Roy, L. Öhrström, *Dalton Trans.* **2015**, *44*, 10156 – 10165; d) A. Karmakar, S. Hazra, M. F. C. Guedes da Silva, A. Paul, A. J. L. Pombeiro, *CrystEngComm* **2016**, *18*, 1337 – 1349; e) A. Karmakar, M. F. C. Guedes da Silva, S. Hazra, A. J. L. Pombeiro, *New J. Chem.* **2015**, *39*, 3004 – 3014; f) A. Paul, A. Karmakar, M. F. C. Guedes da Silva, A. J. L. Pombeiro, *RSC Adv.* **2015**, *5*, 87400 – 87410.

[9] a) R. Jlassi, A. P. C. Ribeiro, M. F. C. Guedes da Silva, K. T. Mahmudov, M. N. Kopylovich, T. B. Anisimova, H. Naïli, G. A. O. Tiag, A. J. L. Pombeiro, *Eur. J. Inorg. Chem.* **2014**, 4541 – 4550; b) R. Nasani, M. Saha, S. M. Mobin, L. M. D. R. S. Martins, A. J. L. Pombeiro, A. M. Kirillov, S. Mukhopadhyay, *Dalton Trans.* **2014**, *43*, 9944 – 9954; c) A. M. Kirillov, M. V. Kirillova, A. J. L. Pombeiro in *Advances in Organometallic Chemistry and Catalysis: The Silver/Gold Jubilee ICOMC Celebratory Book* (Ed.: A. J. L. Pombeiro), Wiley, Hoboken, NJ, **2014**, Part 1, pp. 27 – 38; d) A. Karmakar, L. M. D. R. S. Martins, S. Hazra, M. F. C. Guedes da Silva, A. J. L. Pombeiro, *Cryst. Growth Des.* **2016**, *16*, 1837 – 1849; e) A. Dhakshinamoorthy, M. Alvaro, H. Garcia, *Catal. Sci. Technol.* **2011**, *1*, 856 – 867; f) A. Dhakshinamoorthy, A. M. Asiri, H. Garcia, *Chem. Eur. J.* **2016**, *22*, 8012 – 8024; g) A. Paul, A. P. C. Ribeiro, A. Karmakar, M. F. C. Guedes da Silva, A. J. L. Pombeiro, *Dalton Trans.* **2016**, *45*, 12779 – 12789.

[10] a) S. Horike, M. Dincă, K. Tamaki, J. R. Long, *J. Am. Chem. Soc.* **2008**, *130*, 5854 – 5855; b) A. Dhakshinamoorthy, M. Opanasenko, J. Čejka, H. Garcia, *Adv. Synth. Catal.* **2013**, *355*, 247 – 268.

[11] a) A. Dhakshinamoorthy, M. Alvaro, H. Garcia, *Chem. Eur. J.* **2010**, *16*, 8530 – 8536; b) D. Jiang, T. Mallat, F. Krumeich, A. Baiker, *J. Catal.* **2008**, *257*, 390 – 395.

[12] a) A. Karmakar, G. M. D. M. Rúbio, M. F. C. Guedes da Silva, A. P. C. Ribeiro, A. J. L. Pombeiro, *RSC Adv.* **2016**, *6*, 89007 – 89018; b) C. Chizallet, S. Lazare, D. Bazer-Bachi, F. Bonnier, V. Lecocq, E. Soyer, A.-A. Quoineaud, N. Bats, *J. Am. Chem. Soc.* **2010**, *132*, 12365 – 12377; c) M. Savonnet, S. Aguado, U. Ravon, D. Bazer-Bachi, V. Lecocq, N. Bats, C. Pinel, D. Farrusseng, *Green Chem.* **2009**, *11*, 1729 – 1732; d) M. Pramanik, M. Nandi, H. Uyama, A. Bhaumik, *Green Chem.* **2012**, *14*, 2273 – 2281.

[13] a) S. M. J. Rogge, A. Bavykina, J. Hajek, H. Garcia, A. I. Olivos-Suarez, A. Sepúlveda-Escribano, A. Vimont, G. Clet, P. Bazin, F. Kapteijn, M. Daturi, E. V. Ramos-Fernandez, F. X. Llabrés i Xamena, V. Van Speybroeck, J. Gascon, *Chem. Soc. Rev.* **2017**, *46*, 3134 – 3184; b) *Metal Organic Frameworks as Heterogeneous Catalysts* (Eds.: F. X. Llabrés i Xamena, J. Gascon), The Royal Society of Chemistry, Cambridge, **2013**; c) J. Liang, Z. Liang, R. Zou, Y. L. Zhao, *Adv. Mater.* **2017**, *29*, 1701139.

[14] a) M. N. Kopylovich, A. Mizar, M. F. C. Guedes da Silva, T. C. O. Mac Leod, K. T. Mahmudov, A. J. L. Pombeiro, *Chem. Eur. J.* **2013**, *19*, 588 – 600; b) C. Pettinari, F. Marchetti, A. Cerquetella, R. Pettinari, M. Monari, T. C. O. Mac Leod, L. M. D. R. S. Martins, A. J. L. Pombeiro, *Organometallics* **2011**, *30*, 1616 – 1626; c) M. Shibasaki, M. Kanai, S. Matsunaga, N. Kumagai, *Top. Organomet. Chem.* **2011**, *37*, 1 – 30; d) F. A. Luzzio, *Tetrahedron* **2001**, *57*, 915 – 945; e) S. E. Milner, T. S. Moody, A. R. Maguire, *Eur. J. Org. Chem.* **2012**, 3059 – 3067.

[15] a) R. Ballini, G. Bosica, P. Forconi, *Tetrahedron* **1996**, *52*, 1677 – 1684; b) G. Rosini, R. Ballini, *Synthesis* **1988**, 833 – 847.

[16] a) H. Naïli, F. Hajlaoui, T. Mhiri, T. C. O. Mac Leod, M. N. Kopylovich, K. T. Mahmudov, A. J. L. Pombeiro, *Dalton Trans.* **2013**, *42*, 399 – 406; b) N. Q. Shixaliyev, A. M. Maharramov, A. V. Gurbanov, V. G. Nenajdenko, V. M. Muzalevskiy, K. T. Mahmudov, M. N. Kopylovich, *Catal. Today* **2013**, *217*, 76 – 79; c) N. L. Nkhili, W. Rekik, T. Mhiri, K. T. Mahmudov, M. N. Kopylovich, H. Naïli, *Inorg. Chimi. Acta* **2014**, *412*, 27 – 31; d) K. T. Mahmudov, M. N. Kopylovich, M. Haukka, G. S. Mahmudova, E. F. Esmaeila, F. M. Chyragov, A. J. L. Pombeiro, *J. Mol. Struct.* **2013**, *1048*, 108 – 112; e) M. D. Jones, C. J. Cooper, M. F. Mahon, P. R. Raithbya, D. Apperley, J. Wolowska, D. Collison, *J. Mol. Catal. A: Chem.* **2010**, *325*, 8 – 14.

[17] a) M. Hartmann, M. Fischer, *Microporous Mesoporous Mater.* **2012**, *164*, 38 – 43; b) F. Xamena, F. G. Cirujano, A. Corma, *Microporous Mesoporous Mater.* **2012**, *157*, 112 – 117; c) X. M. Lin, T. T. Li, L. F. Chen, L. Zhang, C.-Y. Su, *Dalton Trans.* **2012**, *41*, 10422 – 10429; d) R. Haldar, S. K. Reddy, V. M. Suresh, S. Mohapatra, S. Balasubramanian, T. K. Maji, *Chem. Eur. J.* **2014**, *20*, 4347 – 4356; e) N. Wei, M. Y. Zhang, X. N. Zhang, G. M. Li, X. D. Zhang, Z. B. Han, *Cryst. Growth Des.* **2014**, *14*, 3002 – 3009; f) L. Ma, X. Wang, D. Deng, F. Luo, B. Ji, J. Zhang, *J. Mater. Chem. A* **2015**, *3*, 20210 – 20217; g) Y. Yang, H.-F. Yao, F.-G. Xi, E.-Q. Gao, *J. Mol. Catal. A: Chem.* **2014**, *390*, 198 – 205; h) S. Srivastava, H. Aggarwal, R. Gupta, *Cryst. Growth Des.* **2015**, *15*, 4110 – 4122; i) M. Y. Masoomi, S. Beheshti, A. Morsali, *J. Mater. Chem. A* **2014**, *2*, 16863 – 16866.

[18] a) E. Knoevenagel, *Ber. Dtsch. Chem. Ges.* **1898**, *31*, 2585 – 2595; b) G. Jones, *Org. React.* **1967**, *15*, 204 – 599; c) E. M. Schneider, M. Zeltner, N. Kränzlin, R. N. Grass, W. J. Stark, *Chem. Commun.* **2015**, *51*, 10695 – 10698; d) Y. Ogiwara, K. Takahashi, T. Kitazawa, N. Sakai, *J. Org. Chem.* **2015**, *80*, 3101 – 3110; e) T. He, R. Shi, Y. Gong, G. Jiang, M. Liu, S. Qian, Z. Wang, *Synlett* **2016**, *27*, 1864 – 1869.

[19] a) J. Park, J. R. Li, Y. P. Chen, J. Yu, A. A. Yakovenko, Z. U. Wang, L.-B. Sun, P. B. Balbuena, H. C. Zhou, *Chem. Commun.* **2012**, *48*, 9995; b) A. Taher, D.-J. Lee, B.-K. Lee, I.-M. Lee, *Synlett* **2016**, *27*, 1433 – 1437; c) Z. Miao, Y. Luan, C. Qi, D. Ramella, *Dalton Trans.* **2016**, *45*, 13917 – 13924; d) F.-G. Xi, H. Liu, N.-N. Yang, E.-Q. Gao, *Inorg. Chem.* **2016**, *55*, 4701 – 4703; e) S. Saravanamurugan, M. Palanichamy, M. Hartmann, V. Murugesan, *Appl.*

Catal. A **2006**, *298*, 8–15; f) S. Hasegawa, S. Horike, R. Matsuda, S. Furu-kawa, K. Mochizuki, Y. Kinoshita, S. Kitagawa, *J. Am. Chem. Soc.* **2007**, *129*, 2607–2614.

[20] a) G. Kumar, H. Aggarwal, R. Gupta, *Cryst. Growth Des.* **2013**, *13*, 74–90; b) G. Kumar, R. Gupta, *Inorg. Chem.* **2015**, *54*, 2603–2615; c) S. Srivasta-va, V. Kumar, R. Gupta, *Cryst. Growth Des.* **2016**, *16*, 2874–2886; d) G. Kumar, R. Gupta, *Inorg. Chem.* **2012**, *51*, 5497–5499; e) J. Park, Y.-P. Chen, Z. Perry, J.-R. Li, H.-C. Zhou, *J. Am. Chem. Soc.* **2014**, *136*, 16895–16901.

[21] a) K. Nakamoto, *Infrared and Raman Spectra of Inorganic and Coordina-tion Compounds, 5th ed.*, Wiley, New York, **1997**; b) G. Socrates, *Infrared Characteristic Group Frequencies*, Wiley, New York, **1980**; c) D. T. Yazıcı, C. Bilgiç, *Surf. Interface Anal.* **2010**, *42*, 959–962; d) V. V. Kumar, G. Naresh, M. Sudhakar, C. Anjaneyulu, S. K. Bhargava, J. Tardio, V. K. Reddy, A. H. Padmasric, A. Venugopal, *RSC Adv.* **2016**, *6*, 9872–9879.

[22] L. Yang, D. R. Powell, R. P. Houser, *Dalton Trans.* **2007**, *955*–964.

[23] a) Y. Jiang, L. Sun, J. Du, Y. Liu, H. Shi, Z. Liang, J. Li, *Cryst. Growth Des.* **2017**, *17*, 2090–2096; b) R. Wang, X. Liu, D. Qi, Y. Xu, L. Zhang, X. Liu, J. Jiang, F. Dai, X. Xiao, D. Sun, *Inorg. Chem.* **2015**, *54*, 10587–10592.

[24] a) X.-M. Lin, T.-T. Li, Y.-W. Wang, L. Zhang, C.-Y. Su, *Chem. Asian J.* **2012**, *7*, 2796–2804; b) J.-M. Gu, W.-S. Kim, S. Huh, *Dalton Trans.* **2011**, *40*, 10826–10829; c) M. Gupta, D. De, S. Pal, T. K. Pal, K. Tomar, *Dalton Trans.* **2017**, *46*, 7619–7627; d) N. M. R. Martins, K. T. Mahmudov, M. F. C.

Guedes da Silva, L. M. D. R. S. Martins, F. I. Guseinov, A. J. L. Pombeiro, *Cat. Commun.* **2016**, *87*, 49–52; e) M. Sutradhar, M. F. C. Guedes da Silva, A. J. L. Pombeiro, *Cat. Commun.* **2014**, *57*, 103–106; f) L.-X. Shi, C.-D. Wu, *Chem. Commun.* **2011**, *47*, 2928–2930.

[25] a) P. Valvekens, M. Vandichel, M. Waroquier, V. V. Speybroeck, D. J. De Vos, *Catal.* **2014**, *317*, 1–10; b) Y. Tan, Z. Fu, J. Zhang, *Inorg. Chem. Commun.* **2011**, *14*, 1966–1970; c) M. Almáši, V. Zeleňák, M. Opanasen-ko, J. Čejka, *Dalton Trans.* **2014**, *43*, 3730–3738.

[26] H. E. B. Lempers, R. A. Sheldon, *J. Catal.* **1998**, *175*, 62–69.

[27] V. J. Bulbule, V. H. Deshpande, S. Velu, A. Sudalai, S. Sivasankar, V. T. Sathe, *Tetrahedron* **1999**, *55*, 9325–9332.

[28] a) Bruker, *APEX2*, Bruker AXS Inc., Madison, Wisconsin, USA, **2012**; b) G. M. Sheldrick, *SADABS, Program for Empirical Absorption Correction*, University of Gottingen, Germany, **1996**; c) G. M. Sheldrick, *Acta Crystal-logr.* **2015**, *C71*, 3–8; d) L. J. Farrugia, *J. Appl. Crystallogr.* **2012**, *45*, 849–854; e) A. L. Spek, *Acta. Cryst.* **2009**, *D65*, 148–155.

[29] CCDC 1813703 (**1**), 1813704 (**2**), and 1813705 (**3**) contain the supple-mentary crystallographic data for this paper. These data can be ob-tained free of charge from The Cambridge Crystallographic Data Centre.